

## Validity of actinometry to measure N and H atom concentration in $N_2$ - $H_2$ direct current glow discharges

This content has been downloaded from IOPscience. Please scroll down to see the full text.

1999 J. Phys. D: Appl. Phys. 32 3208

(<http://iopscience.iop.org/0022-3727/32/24/317>)

View [the table of contents for this issue](#), or go to the [journal homepage](#) for more

Download details:

IP Address: 150.163.34.14

This content was downloaded on 11/11/2015 at 15:13

Please note that [terms and conditions apply](#).

# Validity of actinometry to measure N and H atom concentration in $N_2-H_2$ direct current glow discharges

J C Thomaz, J Amorim and C F Souza

Departamento de Física, Instituto Tecnológico de Aeronáutica, Centro Técnico Aeroespacial, 12228-900-São José dos Campos, Brazil

Received 19 April 1999, in final form 7 September 1999

**Abstract.** The validity of actinometry to measure N and H atoms in nitrogen–hydrogen direct current (dc) glow discharges was investigated. The experiments were conducted in positive columns of dc glow discharges, in mixtures of  $N_2-xH_2$ , where  $x$  varies from zero to one, pressures between 133.33 and 533.32 Pa and discharge currents from 1 to 50 mA. The electric fields were measured by electric probes ( $17 \text{ V cm}^{-1} < E < 32 \text{ V cm}^{-1}$ ), and the gas temperatures ( $490 \text{ K} < T_g < 910 \text{ K}$ ) were deduced from the rotational transitions of molecular-band systems. The actinometry was performed using argon as the actinometer gas and compared with laser induced fluorescence measurements of ground-state atoms, in order to establish the limits of the validity of actinometry. A theoretical approach was used in order to interpret the behaviour of the emission lines. In nitrogen–hydrogen positive columns, the actinometry method indicated the correct behaviour of the N atoms density in the range of zero to one for  $x$  and for H atoms in the region from  $x = 0$  to  $x = 0.2$ .

## 1. Introduction

Electrical discharges in gases have been of great interest in the last few years due to technological applications of plasmas [1]. Among the possible applications of cold plasmas, surface hardening of metals is one important application in the metallurgical industry. Hardening of metals changes the properties of the surface layers without changing the bulk characteristics. One of the most important surface hardening processes is the nitriding of metals in nitrogen–hydrogen discharge mixtures.

Today, it is recognized that one of the most important precursors in gas discharge nitriding is the nitrogen atom and so the study of its production and loss mechanisms is of fundamental importance [2]. Another equally important radical is the hydrogen atom. The role of H atoms seems to be the clean-up of the surface and the control of the white-layer formation [3]. So the detection of these species is very important in order to understand the non-equilibrium kinetics of the medium, as well as to relate them to the properties changed in the surface by the gas discharge.

As was pointed out in recent experimental and theoretical works, the dissociation of the nitrogen and hydrogen in  $N_2-H_2$  glow discharges is coupled to ionization [4, 5, 28]. Therefore, the measurement of these atoms' densities, which are found in the majority in their ground state, is of fundamental importance to describe the kinetics of this medium. In order to detect atoms in the ground state, the most interesting technique is laser induced fluorescence (LIF),

where the fluorescence induced by the laser is related to the ground state atoms' density [6]. Although the technique is very attractive, its application in industrial environments is quite complicated, due to the complexity of the laser systems. This problem can be solved if we employ optical emission spectroscopy (OES), which is a simple technique to implement in industry in a broad range of applications.

Despite the simplicity of OES, it cannot be employed directly in order to probe N and H atoms in their ground state. In fact, OES measurements provide information about the excited electronic states, which are not necessarily related to the density of atoms in the ground state.

Actinometry is an OES technique that uses the addition of a small amount of noble gas in the discharge, in our case argon, in which the intensities of its spectral lines are representative of the excitation mechanism. The comparison of the emitted line intensity by the N or H excited atoms with the intensity of an emitted line of argon, allows one to eliminate the influence of line intensity changes due to excitation conditions and evaluate the real behaviour of the emitted line intensity due to the changes in the ground state atoms' concentration.

Section 2 presents the experimental set-up employed in these OES experiments. The principles of the actinometry technique are revised in section 3, where the choice of the actinometer, the production and loss of excited states as well as the cross section data are discussed. In section 4 the results obtained are presented and in section 5 we present the main conclusions of the present work.

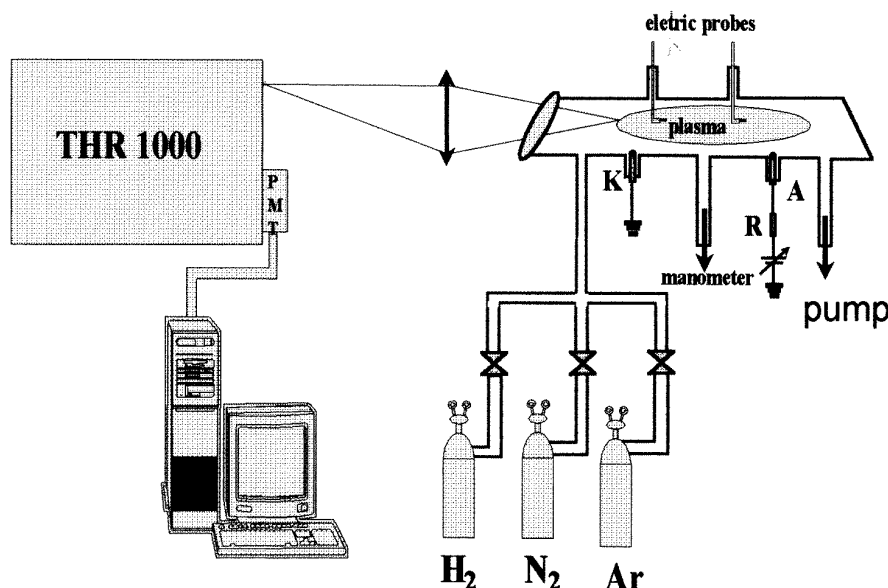


Figure 1. Experimental set-up.

## 2. Experimental set-up

The glow discharge tube has a 16 mm internal diameter and is 20 cm long, see figure 1. Two electric probes, 10 cm apart, are inserted into the positive column, in order to measure the electric field, electron temperature and density. The gases are connected to the discharge tube by means of mass flow controllers, MKS 247C, to make it possible to control the gas discharge mixture. The pressure is measured in the central region of the discharge tube with the aid of a capacitive transducer Baratron. An 8 m<sup>3</sup> h<sup>−1</sup> mechanical pump maintains the flow of the nitrogen–hydrogen gas mixture. The gases employed in the experiments are of ultra-high purity, 99.999%.

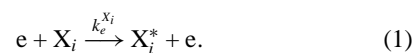
The light emitted by the discharge is focused by means of a lens, 15 cm focal length, into the entrance slit of 1 m monochromator (THR1000) made by Jobin–Yvon. The monochromator is equipped with a grating of 1800 lines mm<sup>−1</sup>, blazed in the region 450–850 nm. The light is colimated at the exit slit where a photomultiplier tube, R928 Hamamatsu, converts photons into an electric signal. The current generated by the photomultiplier tube is sent to a data acquisition electronics Spectralink, where the signal is processed by Spectramax software. The optical system was absolutely calibrated with the aid of a tungsten lamp.

## 3. Principles of actinometry

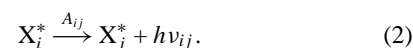
Actinometry is an OES technique, employed when we are interested in the measurements of atoms and molecules in their ground states, but employing emission spectroscopy. It has the advantages of being non-intrusive and having good spatio-temporal resolution.

Although actinometry is a straightforward technique, certain conditions must be satisfied in order to obtain reliable measurements [7, 8]. The first assumption is that both species must be excited to a given state by direct electronic impact

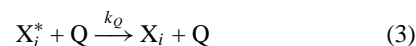
from the ground state,



The de-excitation of the excited states  $X_i^*$  must be radiative,



Therefore, we are assuming a corona equilibrium model for our plasma. In this assumption, cascading processes from higher excited states are not taken into account. However, in our discharge condition the excited state  $X_i^*$  may be quenched by a non-radiative process with species Q,



where Q in this case is Q = N, H, N<sub>2</sub>, H<sub>2</sub>. For the actinometry to be valid, the quenching of the excited state  $X_i^*$  should be a negligible loss term when compared with de-excitation by the radiative process.

To perform actinometry, a small amount of noble gas is introduced in the discharge, taking care that the discharge is not perturbed. The emission intensity of a given line  $I_{X^*}$  of a transition  $X_i^* \rightarrow X_j^*$  may be written as

$$I_{X^*} = C \frac{h\nu_{ij} A_{ij} k_e^{X_i} n_e}{(\sum A_{ij} + k_Q [Q])} [X] \quad (4)$$

where  $n_e$  is the electron density,  $h\nu_{ij}$  is the energy of the emitted photon (relation (2)),  $A_{ij}$  is the Einstein coefficient for the observed transition ( $i \rightarrow j$ ),  $\sum A_{ij}$  is the sum of all radiative de-excitation processes with origin in the  $i$  level,  $k_e^{X_i}$  is the rate coefficient for the transition  $i \rightarrow j$ , and  $k_Q$  is the quenching coefficient. Here C represents a constant that is related to the sensitivity of the detection system.

In order to eliminate the dependence on the  $n_e$  variations, the emitted line intensity may be divided by the intensity of an emitted line of the actinometer, which in our work was the

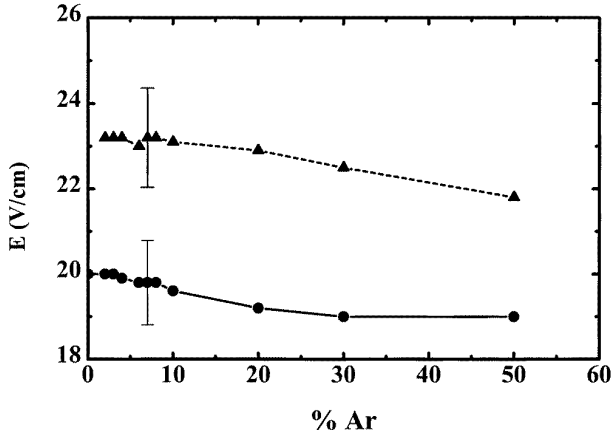


**Figure 2.** Electric field as a function of argon added to the mixture 20% H<sub>2</sub>–80% N<sub>2</sub> (full curve) and 80% H<sub>2</sub>–20% N<sub>2</sub> (dashed curve). The discharge current is 35 mA and the pressure 133.32 Pa.

7503.9 Å line (transition 2p<sub>1</sub> → 1s<sub>2</sub>) of argon. If we suppose, for example, the 7442.3 Å (transition 3p <sup>4</sup>S<sub>0</sub> → 3s <sup>4</sup>P) emitted line of the nitrogen atom, the ratio becomes

$$\frac{I_N^*}{I_{Ar}^*} = \frac{h\nu_{ij}^N A_{ij}^{Ar} k_e^N (\sum A_{ij}^{Ar} + k_Q^N [Q]) [N_2] [N]}{h\nu_{ij}^{Ar} A_{ij}^N k_e^{Ar} (\sum A_{ij}^N + k_Q^N [Q]) [Ar] [N_2]} = \frac{1}{C_N^{Ar}} \frac{[N]}{[N_2]} \quad (5)$$

where

$$C_N^{Ar} = \frac{h\nu_{ij}^{Ar} A_{ij}^{Ar} k_e^{Ar} (\sum A_{ij}^N + k_Q^N [Q]) [Ar]}{h\nu_{ij}^N A_{ij}^N k_e^N (\sum A_{ij}^{Ar} + k_Q^N [Q]) [N_2]}$$

so the ratio  $I_N/I_{Ar}$  is proportional to the  $[N]/[N_2]$  concentration ratio once  $C_N^{Ar}$  is kept constant along the whole ranges of discharge pressure and current. It should be emphasized that  $C_N^{Ar}$  is approximately constant if the energy threshold and the excitation cross sections are similar.

In the next section we present a discussion about the choice of argon as actinometer gas.

### 3.1. Choice of the actinometer

In this study, argon was chosen as actinometer gas because the excitation of the 2p<sub>1</sub> (or 4p' <sup>2</sup>P<sub>1/2</sub>) level is 13.47 eV, a value which is close to the excitation threshold for the 3p <sup>4</sup>S° level of N, which is 13.80 eV, and for the H<sub>α</sub> line (level 3d <sup>2</sup>D<sub>j</sub>) which is 12.06 eV.

The addition of the actinometer should not disturb the discharge. This was verified by measuring the variation of the electric field in the positive column when argon was added to the mixture. As we can see in figure 2, the electric field in the positive column remains constant until 5% Ar is added to the mixture, and drops after this value. In this work, we employed in the actinometry measurements a mixture with 5% Ar. In this figure two situations of discharge mixture are presented: 20% H<sub>2</sub>–80% N<sub>2</sub> (full curve) and 80% H<sub>2</sub>–20% N<sub>2</sub> (dashed curve) for a discharge current of 35 mA and pressure of 133.33 Pa. The behaviour of the electric field is almost the same in these conditions.

Other verification of the influence of argon in the discharge is seen in figure 3. In this figure we can see that until

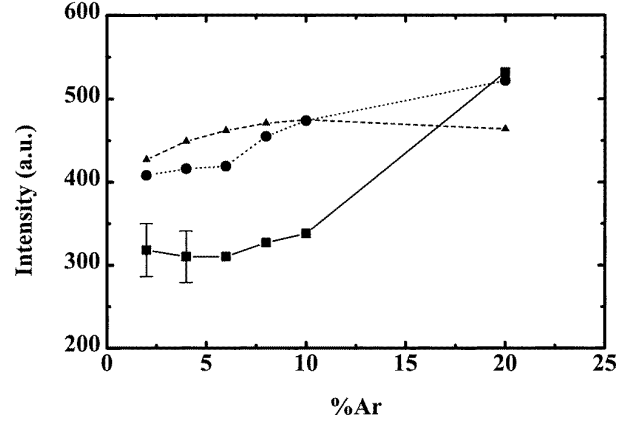


**Figure 3.** Emitted line intensities as a function of argon concentration. H<sub>α</sub> (656.2 nm, dotted curve), N (744.2 nm, dashed curve) and Ar (750.4 nm, full curve). The discharge current is 35 mA and the pressure 133.32 Pa.

**Table 1.** Rate quenching coefficients of argon metastables by nitrogen and hydrogen atoms and molecules.

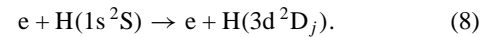
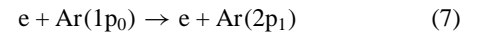
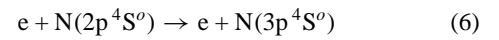
	Ar( <sup>3</sup> P <sub>0</sub> ) ⟨σv⟩ (cm <sup>3</sup> s <sup>−1</sup> )	Ar( <sup>3</sup> P <sub>2</sub> ) ⟨σv⟩ (cm <sup>3</sup> s <sup>−1</sup> )
H	2.2 × 10 <sup>−11</sup> [10]	2.4 × 10 <sup>−10</sup> [10]
H <sub>2</sub>	7.8 × 10 <sup>−11</sup> [11]	6.6 × 10 <sup>−11</sup> [11]
N	1.7 × 10 <sup>−11</sup> [12]	1.7 × 10 <sup>−10</sup> [12]
N <sub>2</sub>	1.6 × 10 <sup>−11</sup> [11]	3.6 × 10 <sup>−11</sup> [11]

the 5% Ar mixture, the intensity of the emitted lines remains approximately constant. For higher argon concentrations, the intensities of the hydrogen and Ar line begin to increase. The intensity of the nitrogen line presents a small increase in this region.

Another important topic is that these excited states must be created by electron impact from the ground state. This statement is justified in the next section on the production and loss of excited states.

### 3.2. Production and loss of excited states

As was stated before, the actinometric measurements are valid if corona equilibrium can be assumed, i.e. the involved excited states should be created by direct electron impact from the ground state. The excitations investigated in this study are:



In the case of argon, the density of the metastables <sup>3</sup>P<sub>0</sub> and <sup>3</sup>P<sub>2</sub> may become important and, as a consequence, the Ar (2p<sub>1</sub>) state may be created from these states by electronic collisions, and the actinometry may become invalid. However, the metastable states of argon, <sup>3</sup>P<sub>0</sub> and <sup>3</sup>P<sub>2</sub>, are efficiently quenched by H<sub>2</sub>, N<sub>2</sub>, N and H, see table 1, and the population of these states in the discharge is negligible [9–12].

Another important remark is that quenching due to collisions of the excited-state atoms with nitrogen and hydrogen molecules may become an important loss factor of these states. A correction factor was then employed in order to take into account this loss channel in the measured emission line intensities:

$$I_{eff} = \left( \frac{\langle \sigma v \rangle_{i, N_2/H_2} n_{N_2/H_2}}{\sum A_{ij}} + 1 \right) I_{meas} \quad (9)$$

where  $I_{eff}$  is the effective intensity of the emitted line and  $I_{meas}$  is the measured intensity.  $\langle \sigma v \rangle_{i, N_2/H_2}$  is the quenching coefficient of excited states by N<sub>2</sub> or H<sub>2</sub>. The quenching coefficient for the argon upper state, 2p<sub>1</sub>, by H<sub>2</sub> is taken from [13] to be  $2.7 \times 10^{-11} \text{ cm}^3 \text{ s}^{-1}$ . The quenching of this state by N<sub>2</sub> is equal to  $3.2 \times 10^{-11} \text{ cm}^3 \text{ s}^{-1}$  [14]. The quenching coefficients of the upper excited state of H ( $n = 3$ ) by H<sub>2</sub>, N<sub>2</sub> and Ar is respectively  $1.8 \times 10^{-9} \text{ cm}^3 \text{ s}^{-1}$ ,  $2.5 \times 10^{-9} \text{ cm}^3 \text{ s}^{-1}$  and  $3.8 \times 10^{-10} \text{ cm}^3 \text{ s}^{-1}$  [15].

In the case of the nitrogen upper state 3p <sup>4</sup>S<sub>0</sub>, the quenching coefficient is not known, so the same values of the H ( $n = 3$ ) is assumed. In this study the quenching of excited states of argon, hydrogen and nitrogen by N and H atoms are discarded due to the low dissociation values in our experimental conditions [16].

### 3.3. Theoretical model and cross section data

In order to interpret our measurements, a theoretical work was undertaken with the aid of the BOLSIG code [17]. The BOLSIG code is a solver for the homogenous Boltzmann equations for electrons, employing the two-term expansion approximation. In this work, this code was used to calculate the coefficients for the excitation of Ar, N and H levels as a function of gas discharge mixture, pressure and current.

In order to study the excitation of the related excited states, we calculated excitation coefficients, using as input parameter the  $E/N$  value measured in each mixture composition. The cross sections for the excitation of the 3p <sup>4</sup>S<sub>0</sub> state of nitrogen was taken from [18]. For argon excitation, the cross section data were taken from [19] and for excitation of the H<sub>α</sub> line by direct impact, the cross section used was obtained from [20]. The cross section for the dissociative excitation of the H<sub>α</sub> line was taken from [21].

## 4. Results

After the presentation of the actinometry principles and discussion about the theoretical model and cross section data employed in this work, we are able to analyse the main results obtained.

The reduced electric field,  $E/N$ , and the electronic density,  $n_e$ , as a function of the hydrogen added to the mixture are presented in figure 4. Two Langmuir probes inserted in the positive column, 10 cm apart, measured the electric field. The density of neutrals  $N$  was determined by the perfect-gas law, where the temperature was estimated from the rotational transitions of molecular band systems. The first system investigated was the second positive system of nitrogen [22] (transition C <sup>3</sup>Π<sub>u</sub> → B <sup>3</sup>Π<sub>g</sub>) for a gas discharge

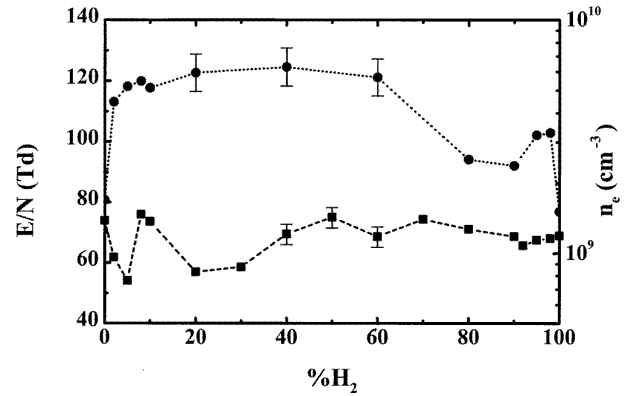


**Figure 4.** Reduced electric field  $E/N$  (dotted curve) and electron density  $n_e$  (dashed curve) as a function of hydrogen added to the mixture. Pressure 266.66 Pa, current 50 mA.

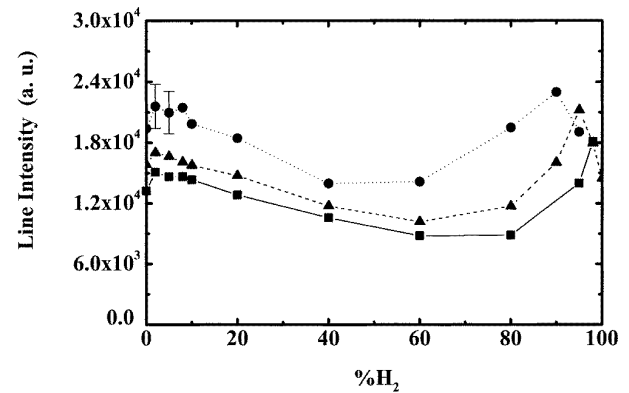


**Figure 5.** Argon line intensity (750.4 nm) as a function of pressure and hydrogen concentration in the mixture. Dotted curve, 133.33 Pa, dashed curve, 266.66 Pa, full curve, 533.32 Pa. Discharge current 50 mA.

mixture of N<sub>2</sub>- $x\%$  H<sub>2</sub>, with  $0 < x < 50$ . For  $x > 50$  the system G <sup>1</sup>Σ<sub>g</sub><sup>+</sup> → B <sup>1</sup>Σ<sub>u</sub><sup>+</sup> of hydrogen was employed [16, 23].

The electron density was measured by one of the Langmuir probes, which may make the validity questionable, at a gas pressure of 133.32 Pa, just to give us an insight into the densities found in the positive column and its behaviour as a function of the discharge parameters.

When a small amount of H<sub>2</sub> is added to N<sub>2</sub>, N<sub>2</sub> (A <sup>3</sup>Σ<sub>u</sub><sup>+</sup>) and N<sub>2</sub> (a' <sup>1</sup>Σ<sub>u</sub><sup>-</sup>) metastable states of nitrogen, which are responsible for the ionization, are destroyed by quenching collisions with H<sub>2</sub> and N<sub>2</sub> [24, 25, 29]. In order to maintain the discharge current constant, an increase in the electric field is necessary to compensate for the loss of the charged particles. As we can see in figure 4, the  $E/N$  has a jump for values between 0% and 5% H<sub>2</sub>, remaining constant for values from 5% to 60% H<sub>2</sub>.

Another  $E/N$  peak is obtained for a gas discharge mixture of 95% H<sub>2</sub>-5% N<sub>2</sub>, probably due to the freezing of the electron energy distribution function, when N<sub>2</sub> is added to the discharge [25], if we are going from the right to the left. The electron density  $n_e$ , decreases when  $E/N$  increases, for an H<sub>2</sub> admixture of 0-5%, see figure 4.

Figure 5 shows the argon emitted line intensity as a function of hydrogen in the mixture. When a small amount

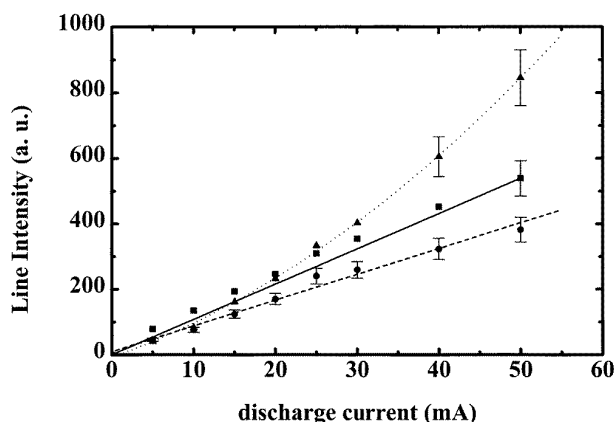
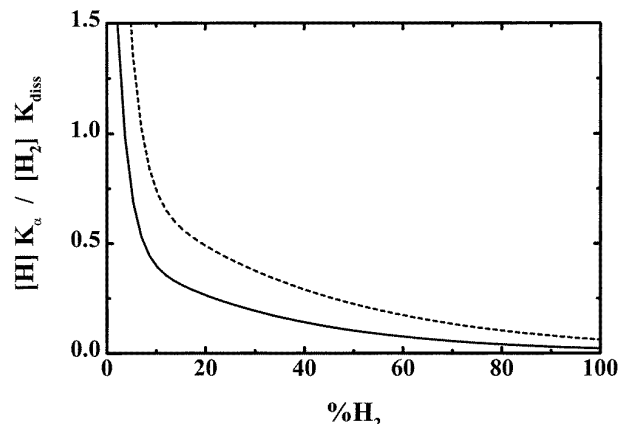


**Figure 6.** Emitted line intensities as a function of discharge current.  $H_{\alpha}$  (656.2 nm, dotted curve), N (744.2 nm, dashed curve), Ar (750.4 nm, full curve). The discharge pressure is 133.33 Pa with a mixture of 20%  $H_2$ –80%  $N_2$ .

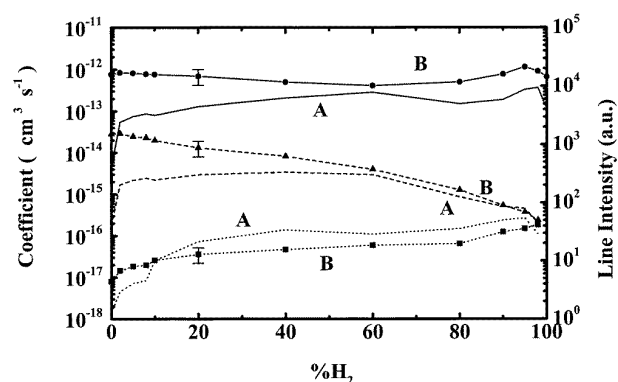
of hydrogen is added to the mixture, a small increase in the emitted line intensity is observed. This may be explained by the increase of  $E/N$  in this region, see figure 4. This figure also shows that for a mixture composition of 90%  $H_2$ –10%  $N_2$  and a pressure of 133.33 Pa, a peak in the emitted line intensity is obtained. For pressures of 266.66 Pa and 533.32 Pa the emitted line intensity peaks move into the region of low concentration of nitrogen in the mixture as the pressure increases. These effects are also due to  $E/N$  increase in this region, see figure 4.

Figure 6 presents the intensity of the following line emissions as a function of the discharge current: the 7503.9 Å line (transition  $2p_1 \rightarrow 1s_2$  of argon), the 7442.3 Å line (transition  $3p^4S_0 \rightarrow 3s^4P$  of nitrogen) and the 6562.8 Å line (transition  $3d^2D_j \rightarrow 2p^2P^o$  of hydrogen). As we can see, the intensity of the 7503.9 Å line (Ar) and of the 7442.3 Å line (N) increase linearly with the discharge current, indicating that the upper excited states in these cases are created by direct electronic impact. The intensity of the 6562.8 Å line as a function of the discharge current, represented in the same figure, shows a different behaviour from the Ar and N lines. It presents a linear increase for discharge currents from 0–20 mA and an exponential growth after 20 mA, showing that in the region 0–20 mA the dissociative pathway for the production of  $H(n = 3)$  atoms may be neglected.

In order to investigate this effect, we have plotted in figure 7 the variations of the direct excitation process rate to the dissociative excitation process rate leading to the production of  $H(n = 3)$  as a function of % $H_2$ , with the aid of the BOLSIG code, see section 3.3. The H atom densities were taken from [26] and the cross sections for direct and dissociative excitation from [20, 21]. As the H atom densities were measured with a precision that was greater than 20% and considering the uncertainties in the measurements of cross sections, we simulated two situations. The first one (full curve) is when the ratio  $H K_{\alpha}/H_2 K_{diss}$  is a function of % $H_2$  and the second is when the ratio  $H K_{\alpha}/H_2 K_{diss}$  is multiplied by two (dashed curve). By these curves, we can expect that actinometry will be critical for large amounts of  $H_2$  in the mixture, but can be employed when the percentage of  $H_2$  in the mixture is low.



**Figure 7.** The ratio of direct excitation to the dissociative excitation of the  $H_{\alpha}$  line as a function of the % $H_2$  in the mixture multiplied by one (full curve) and multiplied by two (dashed curve). Discharge current 50 mA, pressure 266.66 Pa.



**Figure 8.** Calculated excitation coefficient (A) and measured line intensities (B) as a function of hydrogen added to the gas discharge mixture. Argon (750.4 nm, full curves), nitrogen (744.2 nm, dashed curve) and  $H_{\alpha}$  (656.2 nm, dotted curve). Discharge current 50 mA, pressure 266.66 Pa.

The dissociative pathway is largely dominating along the discharge current and pressure for pure hydrogen discharges, invalidating the actinometry method for measuring H atom density, as was observed by St-Onge and Moisan in microwave discharges [27]. However, in mixtures where the percentage of  $H_2$  is varying, this may not be the case for the low concentration of hydrogen.

The coefficient for excitation of the 7503.9 Å (Ar), 7442.3 Å (N) and the 6562.8 Å (H) lines and the emitted line intensities as a function of % $H_2$  are presented in figure 8. As we can see in this figure, the excitation coefficients of all lines increase when  $H_2$  is added to  $N_2$ . This is related to the increase in the electric field, see figure 4. For values of 5–90% of  $H_2$  in the mixture, a plateau is obtained for these three coefficients. For mixtures  $N_2$ – $x\%$   $H_2$  with  $x > 90$ , a small peak is obtained for an  $x$  of about 95% in the three lines, which is related to the increase in the electric field, also observed in figure 4. This behaviour is also observed in the emitted intensity of the 7503.9 Å line of Ar and in the intensity of the  $H_{\alpha}$  line, as we can see in the same figure. However, the intensity of the 7442.3 Å line of the nitrogen atom is always decreasing in intensity as a function of % $H_2$ .

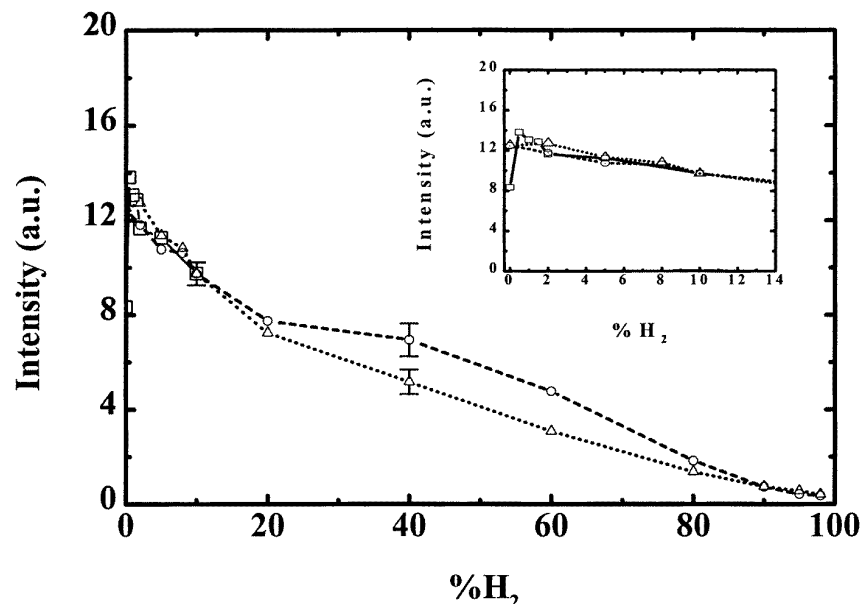


**Figure 9.** Nitrogen atom concentration as a function of hydrogen in the mixture. Squares, LIF signal [28]; open triangles, emission line intensity; open circles, actinometry. Discharge current 50 mA, pressure 266.66 Pa.

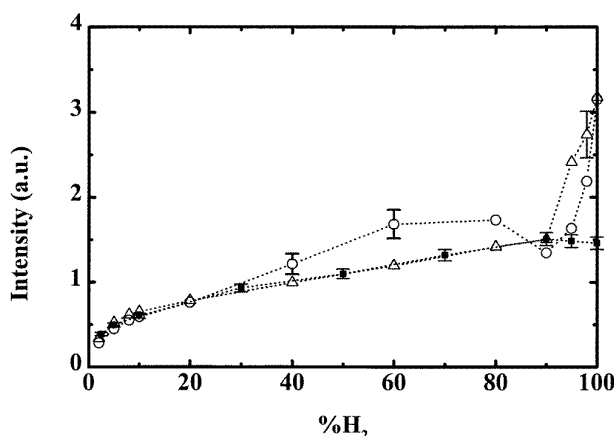


**Figure 10.** Hydrogen atom concentration as a function of hydrogen in the mixture. Squares, LIF signal [28]; open triangles, emission line intensity; open circles, actinometry. Discharge current 50 mA, pressure 266.66 Pa.

The LIF, actinometry and line emission intensity of N atoms are plotted in figure 9. The insert shows the signals enlarged. The LIF points were taken from [28]. It should be mentioned that LIF signals are directly related to the concentrations of N [29] and H [6] atoms in their ground state. In the range where the LIF probe of N atoms was carried out, i.e. up to 14% of  $H_2$  in  $N_2$ , the agreement between the LIF, actinometry and line emission intensity are very good.

Actinometry intensity is higher than emission line intensity in the region 20–80% of  $H_2$  in  $N_2$ . Further experiments using LIF as diagnostic should be desirable, in order to interpret this difference.

The LIF, actinometry and line emission intensity of H atoms are plotted in figure 10. We can see that LIF and line emission intensity are in good agreement in the region 0–90% of  $H_2$  in the mixture, as was presented in [28].

However, by the reason explained above, the contribution of the dissociative pathway in the production of  $H(n=3)$  atoms invalidate the actinometry for H atoms for  $x > 20\%$ . As we can see in figure 7 in the range  $0 < x < 20$ , the ratio of production of  $H(n=3)$  by direct and dissociative pathways varies abruptly. Figure 10 shows that the LIF, actinometry and line intensity have a reasonable agreement in  $N_2-H_2$  discharges only in the region  $N_2-x\% H_2$ , with  $0 < x < 20$ .

## 5. Conclusions

As a conclusion we can state that actinometry was investigated in this work in order to probe N and H atoms in the  $N_2-H_2$  discharge mixture. A study of the actinometry method was undertaken and the limits of this technique were established in our experimental conditions.

For detection of N atoms, actinometry can be applied in the whole mixture range, although LIF diagnostic, in the region 20–80% of  $H_2$  in the mixture, should be desirable, in order to verify the validity of actinometry.

The detection of H atoms in the positive column by actinometry may be used only in the region  $N_2-x\% H_2$ , with  $0 < x < 20$ , because the contribution of  $H(n=3)$  line emission from the dissociative pathway invalidates this diagnostic method for higher concentrations of  $H_2$  in the mixture. However, LIF and line emission intensity have good agreement in the region  $N_2-x\% H_2$ , with  $0 < x < 90$ .

## Acknowledgments

This work was supported in part by Fundação de Amparo à Pesquisa do Estado de São Paulo-Fapesp, under the Young Scientist Program in Emerging Centres (contract numbers 96/10475-9, 97/13288-8 and 97/05712-4).

## References

- [1] Grill A 1994 *Cold Plasma in Materials Fabrication* (Piscataway, NJ: IEEE)
- [2] Ricard A, Gordiets B F, Pinheiro M J, Ferreira C M, Baravian G, Amorim J, Bockel S and Michel H 1998 *Eur. Phys. J. Appl. Phys.* **4** 87
- [3] Szabo A and Wilhelm H 1984 *Plasma Chem. Plasma Proc.* **4** 89
- [4] Gordiets B, Ferreira C M, Pinheiro M J and Ricard A 1998 *Plasma Sources Sci. Technol.* **7** 363
- [5] Gordiets B, Ferreira C M, Pinheiro M J and Ricard A 1998 *Plasma Sources Sci. Technol.* **7** 379
- [6] Amorim J, Baravian G, Jolly J and Touzeau M 1994 *J. Appl. Phys.* **76** 1487
- [7] Pagnon D, Amorim J, Nahorny J, Touzeau M and Vialle M 1995 *J. Phys. D: Appl. Phys.* **28** 1856
- [8] Gicquel A, Chenevier M, Hassouni Kh, Tserepi A and Dubus M 1998 *J. Appl. Phys.* **83** 7504
- [9] Schulz-von der Gathen V and Döbele HF 1996 *Plasma Chem. Plasma Proc.* **16** 461
- [10] Sadeghi N and Setser D W 1985 *Chem. Phys.* **95** 305
- [11] Piper L G, Velazco J E and Setser D W 1973 *J. Chem. Phys.* **59** 3323
- [12] Piper L G, Clyne M A A and Monkhouse P B 1980 *J. Chem. Phys.* **51** 107
- [13] Francis A, Czarnetzki U, Döbele H F and Sadeghi N 1998 *Eur. Phys. J. Appl. Phys.* **4** 239
- [14] Sadeghi N 1999 Private communication
- [15] Preppernau B L, Pearce K, Tserepi A, Wurzburg E and Miller T A 1995 *Chem Phys.* **196** 371
- [16] Amorim J, Loureiro J, Baravian G and Touzeau M 1997 *J. Appl. Phys.* **82** 2795
- [17] BOLSIG (Shareware), Kinema Software (web site: <http://www.csn.net>)
- [18] Ganas P S 1973 *J. Chem. Phys.* **59** 5411
- [19] Puech V and Torchin L 1986 *J. Phys. D: Appl. Phys.* **19** 2309
- [20] Buckman S J and Phelps A V 1985 *JILA Information Center Report* No 27
- [21] Lavrov B P 1977 *Opt. Spectrosc.* **42** 250
- [22] Nahorny J 1994 *PhD Thesis* Université Paris XI, Orsay, France
- [23] Amorim J 1994 *PhD Thesis* Université Paris XI, Orsay, France
- [24] Loureiro J and Ricard A 1993 *J. Phys. D: Appl. Phys.* **26** 163
- [25] Garscadden A and Nagpal R 1995 *Plasma Sources Sci. Technol.* **4** 268
- [26] Amorim J, Baravian G and Sultan G 1996 *Appl. Phys. Lett.* **68** 1915
- [27] St-Onge L and Moisan M 1994 *Plasma Chem. Plasma Proc.* **14** 87
- [28] Bockel S, Amorim J, Baravian G, Ricard A and Stratil P 1996 *Plasma Sources Sci. Technol.* **5** 567
- [29] Amorim J, Baravian G and Ricard A 1995 *Plasma Chem. Plasma Proc.* **15** 721